



Shahrood University of
Technology



Iranian Society of
Mining Engineering
(IRSM)

Compressional and Shear Interval Velocity Modeling to Determine Formation Pressures in an Oilfield of SW Iran

Pooria Kianoush¹, Ghodratollah Mohammadi*¹, Seyed Aliakbar Hosseini², Nasser Keshavarz Faraj Khah³, and Peyman Afzal¹

1. Department of Petroleum and Mining Engineering, South Tehran Branch, Islamic Azad University, Tehran, Iran

2. Department of Petroleum, Materials and Mining Engineering, Central Tehran Branch, Islamic Azad University, Tehran, Iran

3. Deputy Manager Geoscience Faculty, Research Institute of Petroleum Industry (RIPI), Tehran, Iran

Article Info

Received 2 July 2022

Received in Revised form 26 July 2022

Accepted 11 August 2022

Published online 11 August 2022

DOI:10.22044/jme.2022.12048.2201

Keywords

Seismic analysis

Seismic velocity modeling

Compressional velocity cube

Acoustic impedance inversion

Formation pressure

Abstract

In the seismic methods, estimation of the formation pressures is obtained by converting the seismic velocity to the pore pressure, and comparing it with the effective pressure during the well-test program. This work is a new challenge regarding the velocity study domain in an oil field in SW Iran. The reservoir generally consists of carbonate rocks, and contains no shale interbeds. Here, 23 well information, seismic data interpretation, compressional (V_p), and shear velocity (V_s) models are implemented. The models are determined from the combined geo-statistical methods, and the results obtained are compared with the fractal models. The final V_s cube is modeled in order to determine the formation fracture pressure using the exploratory well cores and dipole sonic imager (DSI) V_s logs with a correlation coefficient of 0.95 for the V_s data obtained from the porosity, lithology, and primary DSI data. The vertical seismic profiling (VSP) data introduce a maximum interval velocity of 2760-2900 m/s in the field related to the Gotnia formation. The final amounts of seismic acoustic impedance inversion (AI) at the bottom of the field are mostly in the range of 8000-15000 [(m/s)*(g/cm³)], which can be related to the calcareous formations. Based on the Logratio matrix obtained from the fractal velocity-volume (V_p - V) model, the maximum overall accuracy (OA) in the dominant limestone intervals is 0.74. It indicates a high correlation of the V_p cube model obtained from the combination of sequential Gaussian simulation (SGS) and co-kriging models with AI. The uncertainty studies of V_p model in blind wells are about 50%, which is acceptable considering the large well numbers.

1. Introduction

Understanding the pore pressure of the formation is essential for wells' safe and economical drilling and assessing the exploration risk factors such as fluid migration and sediment integrity. Usually, before drilling, an initial estimate of the pore pressure from the surface seismic data is made by seismic velocities. Then an estimate of the pore pressure is obtained by converting the velocity to the effective pressure suitable for the desired area along with the overburden pressure. The seismic data is the only method to predict the pore pressure in the pre-drilling stage. The seismic methods estimate the pore pressure based on the effect of wave velocity from the pressure changes [1, 2].

The main methods of these studies include velocity modeling to estimate the pore pressure using a combination of seismic data and well information, and compare their accuracy and efficiency [3, 2]. In the seismic methods, pore pressure estimation is obtained by converting the seismic velocity to pore pressure, and comparing it with the pressure obtained during the well test program. The results are determined from geo-statistical or intelligent models such as artificial neural networks [4, 2]. The effective stress cube is produced using the Bower's method's relationship between velocity and effective pressure. Then with the relationship between density and overburden

✉ Corresponding author: ghodratollah46@gmail.com (Gh. Mohammadi).

pressure, the overburden pressure cube is produced [1]. Sonic log (DT)¹ is one of the most important well logs, which can be estimated using other diagrams and artificial neural network methods with acceptable approximation to design drilling fluids such as mud and cement density. Without the necessary information in a part of the field, the necessary graphs are prepared using the estimating models after screening the available data and preparing the database [5, 6]. One way to control the values of the sonic logs is to match them with the values obtained from the seismic velocity analysis. The acoustic log can be a good indicator of the internal pressure of the earth, i.e. increasing the passage time in the zones is a function of changing the porosity or increasing the pore pressure gradient, so it is possible to identify areas with abnormal pore pressure and decrease drilling risk. Because in addition to pressure, other factors such as lithology also affect the speed of seismic waves, therefore, use of the existing geological information and well-surveying logs can largely prevent errors in estimating the pressures of the formation, especially in carbonate formations [3, 1, 7, 8]. For estimating the formation fracture pressure, it is necessary to calculate the shear velocity. Determining the shear wave velocity by the methods such as core analysis requires a lot of time and money. Due to the lack of sufficient cores, lithological changes, and reservoir heterogeneity, determining this parameter by conventional methods is not very accurate. There are also many experimental relationships in the calculation of shear wave velocities, the most widely used of which is the method proposed by Castagna (1993) based on lithological changes [9, 10]. The intelligent methods are one of the new, low-cost, and accurate methods that can be used. Using petrophysical graphs such as DSI estimate the shear wave velocity of the reservoir in the shortest possible time [11]. For estimating the pore pressure with velocity data, the relationship between effective stress and velocity in sediments under normal pressure has been proposed by Bowers (1992):

$$V = V_0 + A\sigma^B \quad (1)$$

$$\sigma = \left[\frac{V - V_0}{A} \right]^{\frac{1}{B}} \quad (2)$$

where V_0 is the velocity of unconsolidated fluid-saturated sediments, and A and B describe the variation in velocity with increasing effective stress (σ), and can be derived from offset well data [12, 13].

In order to calculate the effective pressure in the reservoir area using the Bowers relation, the relation coefficients must first be obtained. Thus according to the effective pressure information at wells (MDT/RFT/DST)² and the overburden pressure cube created in the previous section, the effective stress at points of these wells can be calculated.

Sequential Gaussian simulation (SGS) is typical in geo-statistical simulations, and in many simulators, it has responded to porosity, permeability, and other regional variables. In this method, the simulated value at each point is obtained using the probability distribution function calculated from the raw data and the previous simulation data in the nearest neighbors of the desired point. The first principle in all the Gaussian methods is the normality of the raw data; otherwise, they must become the standard [14, 15]. In the co-kriging method, the evaluation is performed using the correlation between the desired regional variable and the auxiliary variable in places with a shortage of samples. If the correlation between the two variables is greater than 0.5, the estimation error is significantly reduced by this method [16, 17].

The fractal geometry methods are mainly used to analyze complex shapes of geological structures, especially in structural geology and engineering branches, and the separation of geochemical and mineralogical communities, especially in economic geology, mining, and geophysics. Grade-area, grade-number, and power-area spectrum methods are very useful in earth sciences. Mandelbrot (1983) and Agterberg (1995) have proposed a value-size method for determining the threshold values and geochemical background. Hassanpour and Afzal (2013) by drawing a logarithmic diagram of grade-volume wherever the slope of the curve has changed drastically, i.e. the statistical population has changed. That indicates a sharp change in grade and a function of changing geological and mineralization conditions. The formula of the grade-volume method is as follows [18-20]:

$$V(\geq \rho) \propto \rho^{-D} \quad (3)$$

¹ Delta T Sonic Transit Time (us/ft.)

² Modular Dynamic Tester (MDT)/ Repeat Formation Test (RFT)/Drill Stem Test (DST)

In this case, V is the volume that includes larger and equal grades ρ in the studied deposit, and D is the fractal dimension [19, 20]. In this research work, a new challenge is studied to study the compressive velocity by the fractal Velocity-Volume (Vp-V) method.

A logarithmic matrix is used to investigate the overall accuracy between the geological and mathematical models. This matrix was first proposed by Caranza (2011) in gold anomalies caused by stream sediments in the NW Philippines. A 2-by-2 matrix is used to do this. Any data with the highest overlap has the results of geological and mathematical models after calculating the overall accuracy (OA) can be considered a definite result with the least amount of error [21]. In the studied area located in the south Azadegan field, out of 42 wells available, 23 wells have the most selected information, of which 17 wells located in the central, western, and the southern parts have effective pressure test data in the Ilam to Fahliyan reservoir formations. It is discontinuous but this data does not exist in the side-sections of the field, and to calculate the pore pressure gradient in the whole field, this log must be estimated for the wells located in the side sections. For this purpose, by determining the relationships between the existing reservoir data, the initial data cube with geo-statistical methods such as Sequential Gaussian Simulations (SGS) and co-kriging with the same coordinates and inverse distance method has been modeled. The reservoir data includes the

parameters such as compressional and shear velocity, density, gamma, porosity and fluid saturation logs, interval seismic migration velocity, and acoustic impedance resulting from seismic inversion. The South Azadegan field formations are modeled with a simple network of Petrel 2016 software.

2. Material and methods

2.1. Structural geology model based on seismic and geological data

The Azadegan dome is a complex horst. The seismic data of the Azadegan structure show steep faulting in the core of the anticline. These faults die upsection in the Upper Jurassic Gotnia formation. The drill-hole and seismic data from the Azadegan anticline demonstrate unconformities and erosional surfaces due to the uplifting of basement-cored horsts [22], for example, incised channels in the top Cenomanian-Turonian Sarvak formation indicate erosion of the anticline crest in the upper Cretaceous. The location of the structural section is pointed in Figure 1. In this cross-section, the Azadegan structure is presented as a nearly symmetric gentle relief with 3° and 1° eastern and western flanks, respectively. Figure 1(b) shows thinning of both the Mid Cretaceous Bangestan group and the late Cretaceous Gurpi formation in the crest of the Azadegan anticline. It reflects the activity of the Azadegan anticline during the mid- and late Cretaceous [23].

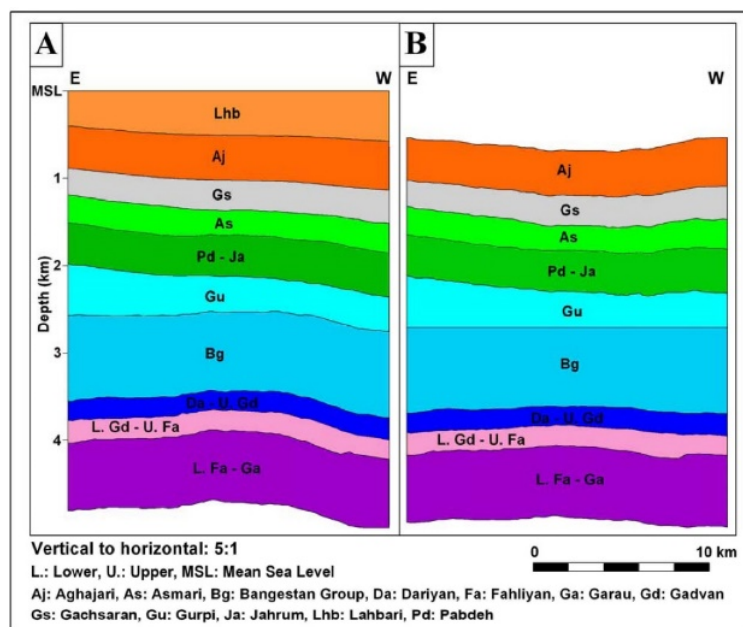


Figure 1. a) A structural cross-section of Azadegan anticline in E-W direction, b) Structural cross-section is flattened at the top Bangestan Group [23].

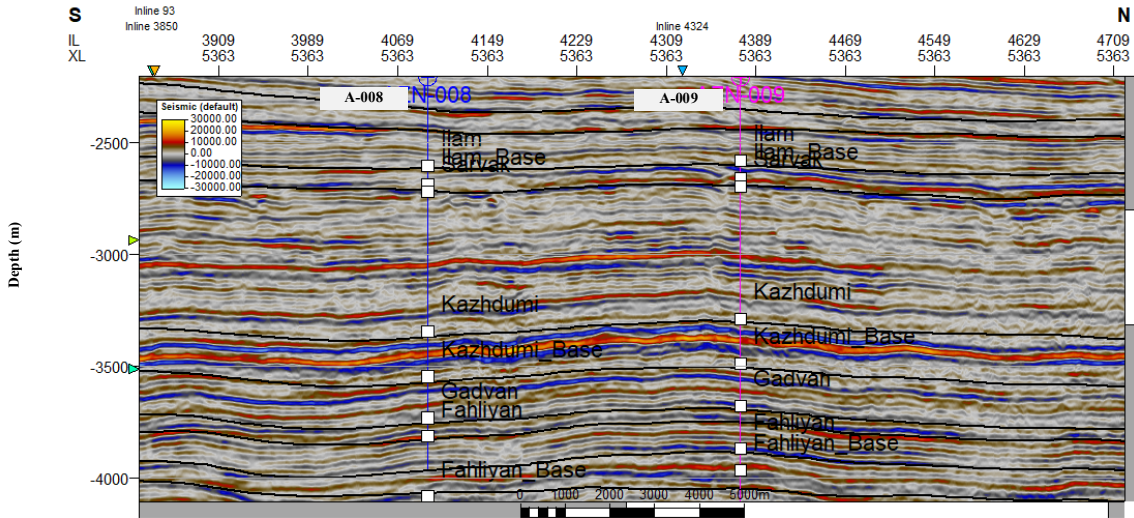


Figure 2. Sample of seismic data section with formation top, depth domain seismic sections, and location of exploratory wells in South Azadegan field.

The South Azadegan field formations are modeled based on the interpretation of time-domain seismic horizons data, and correlated with geological information obtained from exploratory drilling, and depth-domain seismic horizons have been constructed as separate surfaces from the

surface Aghajari formation to the Gotnia formation (Figures 2 and 3). Due to the lack of complex fault systems in the area, the geological model has been built with a simple network of Petrel 2016 software.

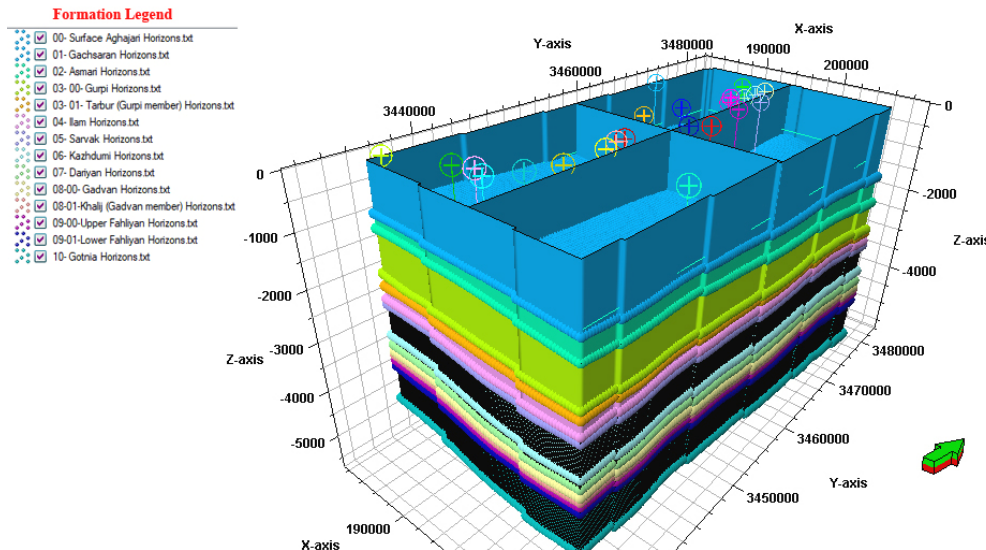


Figure 3. Three-dimensional geological model of South Azadegan field using seismic sections and drilling data along with location of used wells.

2.2. VSP interval velocity model

The interval velocity model was prepared using the relationship between checkshots and Vertical Seismic Profiling (VSP) velocity data and with depth changes in wells with information according to Equation (4), and the coefficients V_0 and K were

determined with a correlation coefficient of 0.95 (Figure 5).

$$V = V_0 + K * Z \tag{4}$$

In this relation, K is the constant conversion factor of change deep horizon layers to the average interval velocity, and V_0 is the surface layer velocity.

The data from Ilam, Sarvak, Kazhdumi, Gadvan, Fahliyan, and Garu formations (from the upper Cretaceous to the Jurassic horizon) has been used to match the data of deep seismic horizons.

$$V = V_0 = V_{int} \tag{5}$$

In order to convert the depth seismic horizon layers to average velocity (Figure 6), due to lack of surface seismic horizon in the surface Aghajari layer used Equation (5) and for other layers from Equation (4) with constant values of $V_0 = 1984.61$ and $K = -0.3721$ calculated according to the table

below. Finally, the average velocity of each formation is calculated using Equation (6), and the average velocity map of each layer is prepared separately; its results are summarized in the table below.

$$V_{avg} \left(\frac{m}{s} \right) = 2000 * Z (m) / TWT (ms) \tag{6}$$

In this formula, TWT is the wave travel time in milliseconds, Z is the depth in meters, and V_{avg} is the average layer velocity in meters per second.

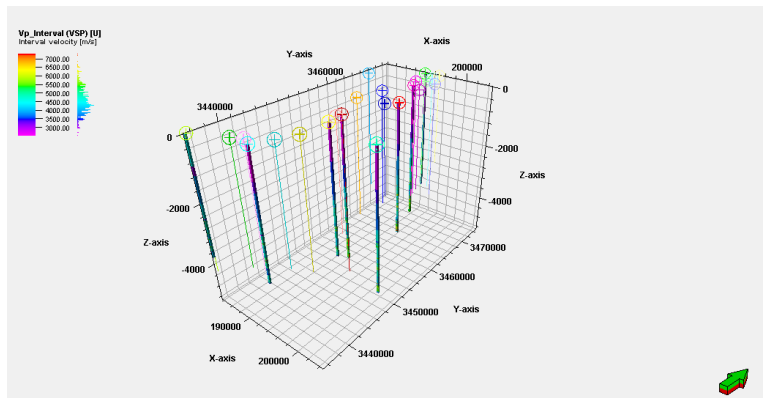


Figure 4. Location of studied wells along with initial model of exploratory wells with VSP data in South Azadegan field.

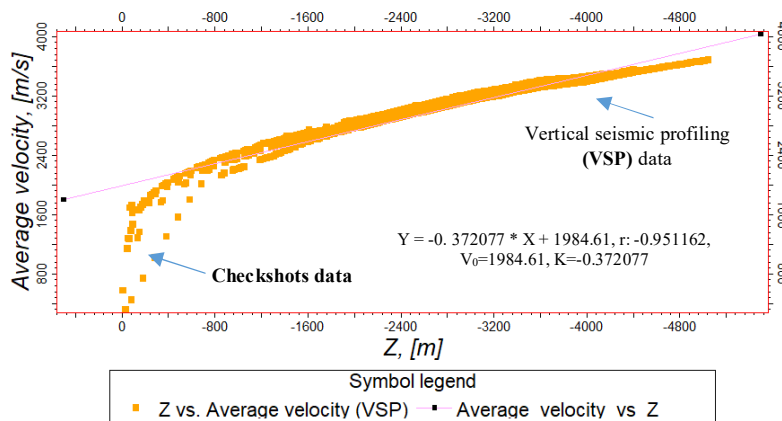


Figure 5. Correlation coefficient of average velocity data of check-shot and VSP points and depth to determine coefficients of velocity model.

Based on this, the average velocity of the surface Aghajari formation with a constant rate of 1984.6 m/s has been calculated, the highest average velocity in the range of 2760- 2900 m/s in the northeast side is related to the Gotnia formation,

and the lowest is related to the Gachsaran formation with 2180-2250 m/s in the southwest direction of the studied area (Table 1). An example of the layer velocity maps in the lower Fahliyan formation is presented in Figure 7.

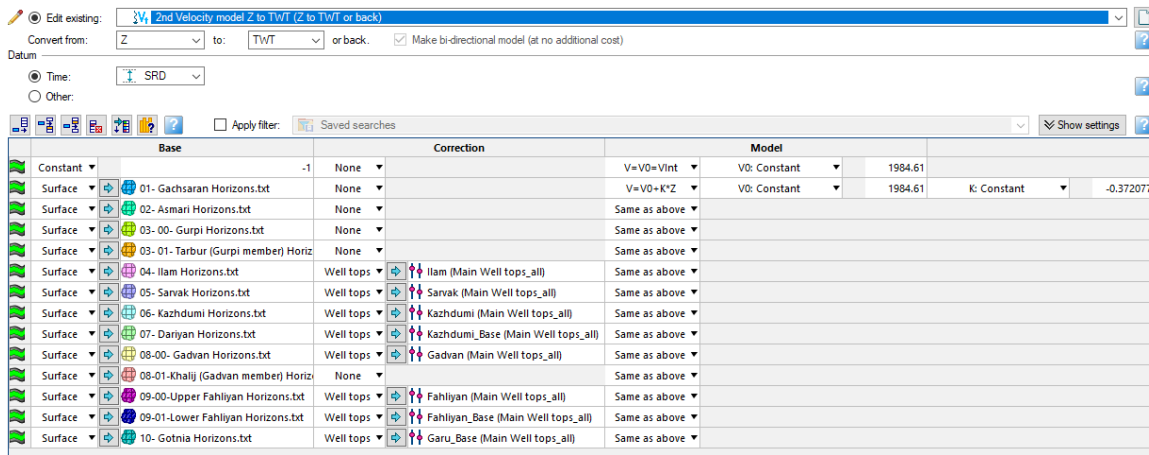


Figure 6. Velocity model based on depth seismic horizon data, formation tops, and VSP-Checkshots data.

According to Figure 7, the average velocity of the lower Fahliyan formation is between 2330 and 2760 m/s, and the highest values of that are visible

in the northeast with red contour and the lowest in the southwest with purple contour.

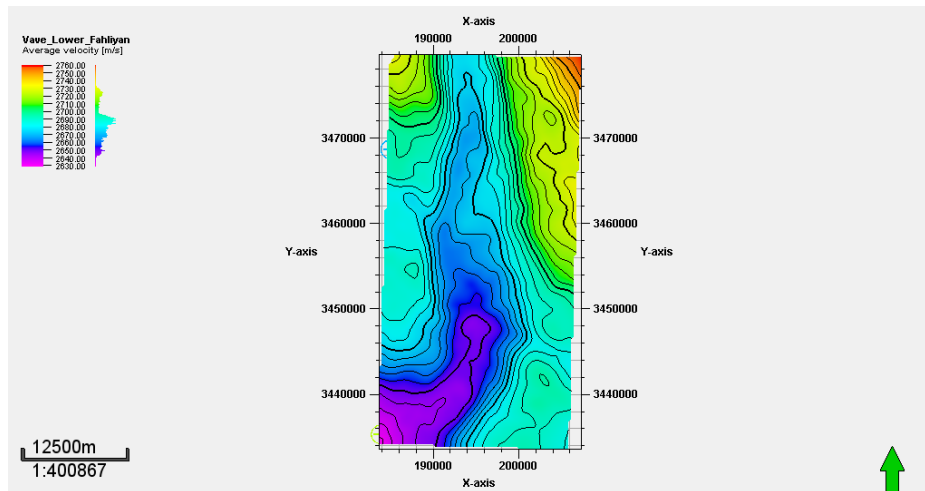


Figure 7. Average velocity map of the lower Fahliyan formation based on seismic horizons and VSP data.

Table 1. Minimum and maximum average layer velocities based on VSP and seismic horizons data.

Formation	Min. V_{avg} (m/s)	Min. V_{avg} direction (degree)	Max. V_{avg} (m/s)	Max. V_{avg} direction (degree)
Aghajari	1984.6	Constant	1984.6	Constant
Gachsaran	2150	Southwest (SW)	2280	Northwest (NW)
Asmari	2200	SW	2340	NE and NW
Gurpi	2330	SW	2460	NE and NW
Tarbur (Member)	2370	SW	2480	NE and NW
Ilam and Laffan	2410	SW	2510	NE and NW
Sarvak	2430	SW	2530	NE and NW
Kazhdumi	2530	SW	2630	NE and NW
Dariyan	2560	SW	2670	NE and NW
Gadvan	2590	SW	2700	NE and NW
Khalij (member)	2600	SW	2710	NE and NW
Upper Fahliyan	2620	SW	2730	NE and NW
Lower Fahliyan to Garu	2630	SW	2760	Northeast (NE)
Gotnia to Neyriz	2760	SW	2900	NE

2.3. Compressional velocity (Vp) model based on sonic log (DT) data

In order to prepare the compressional velocity cube with sonic log (DT) data in the studied field, it was necessary to complete the data for all the wells from the surface to the bottom of each well. Considering that none of the DT logs were taken from the surface, using Artificial Neural Networks (ANN) could not construct the velocity model in the surface layers without information. The surface log data consisted of eight wells with VSP interval velocity, four wells with gamma-ray data from the surface to the bottom of the well, and most of them had density log data. Using the relationships between logs in 5 steps with the highest correlation coefficients, all the 23 exploratory wells studied in the South Azadegan field have complete data of

compressional velocity from the surface to the bottom of the well.

In order to calculate the values of compressional velocity in the first step, by determining the relationship between the “**V (VSP) int**” and “**Gr**” logs, a new log called “**Vp.temp**” was created.

In the second step, using conditional programming in the Petrel 2016 software, another log called “**V2**” was created according to Equation (7) so that at any depth, there is “**Vint(VSP)**” log existed but the **Vp** data was not available (U)¹; “**Vint (VSP)**” is considered equivalent to **Vp**.

The correlation coefficients of VSP and compressional velocity **Vp** were calculated for each of the eight wells separately, and the mean relationship obtained for all wells was used (Table 2).

$$V2=if (V=U, Interval_velocity_VSP, V) \tag{7}$$

Table 2. Correlation coefficients of VSP interval velocity, and compressional velocity (Vp) logs in wells with VSP data.

Well	A-025	A-010	A-006	A-005	A-004	A-002	A-001
Correlation coefficient of VSP and Vp logs	0.8077	0.7323	0.5991	0.5083	0.5433	0.7980	0.5324
Total (r)	Vp = 0.33041 * V _{int} (VSP) + 3139.5, Correlation coefficient: 0.416904						

The initial data log was the sonic delta transmit time (DT) in microseconds per foot (us/ft), which was converted to meters per second (m/s) with Equation (8). Also all out-of-range DT data that had been generated due to noise or error had been removed.

$$V_p \left(\frac{m}{s} \right) = \frac{304,785.13}{DT \left(\frac{\mu s}{ft} \right)} \tag{8}$$

In the third step, by combining the data of “**V2**” and “**Vp.temp**” logs, a new log called “**Vp.full**” was created according to Equation (9) so that the parts without “**V2**” data were completed with “**Vp.temp**” data:

$$Vp_Full=If(V2=U, Vp_temp, V2) \tag{9}$$

In the fourth step, after completing the density data based on the depth changes, another log called **Vp.full2** was prepared based on the relationship between the density and the initial compressional velocity data.

Finally, in the fifth step, “**Vp.full_final**” log was made according to Equation (9), so that where “**Vp.full**” data was not available, “**Vp.full.2**” data was used (Figure 9).

$$Vp_Full_Final=If(Vp_Full=U,Vp_Full2, Vp_Full) \tag{10}$$

Based on “**Vp.full_final**” obtained log, all 23 exploratory wells in the South Azadegan field have complete data of compressional velocity (**Vp**) from the surface to the bottom of the well. Then by developing the model to the whole cube with scaling up, the **Vp** velocity cube model builds in the next step (Figure 8).

¹ U: Undefined

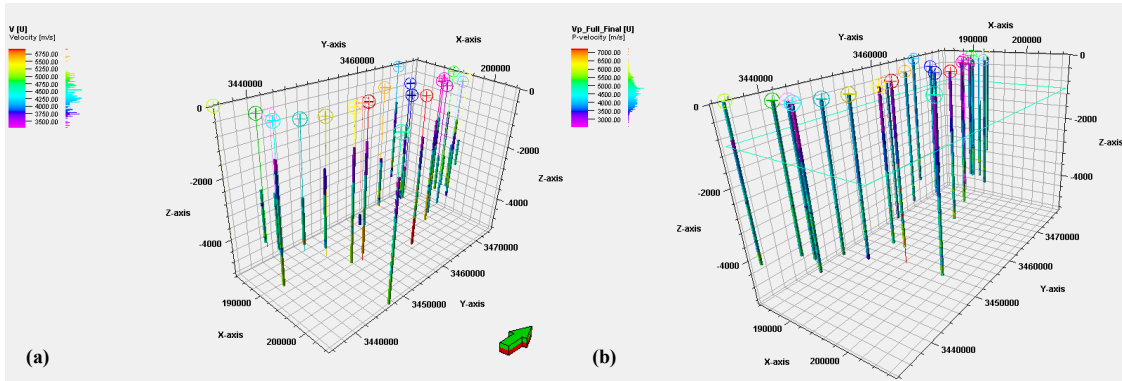


Figure 8. Scaled up velocity model a) initial "Vp" log and b) final "Vp.full_final" log in studied area.

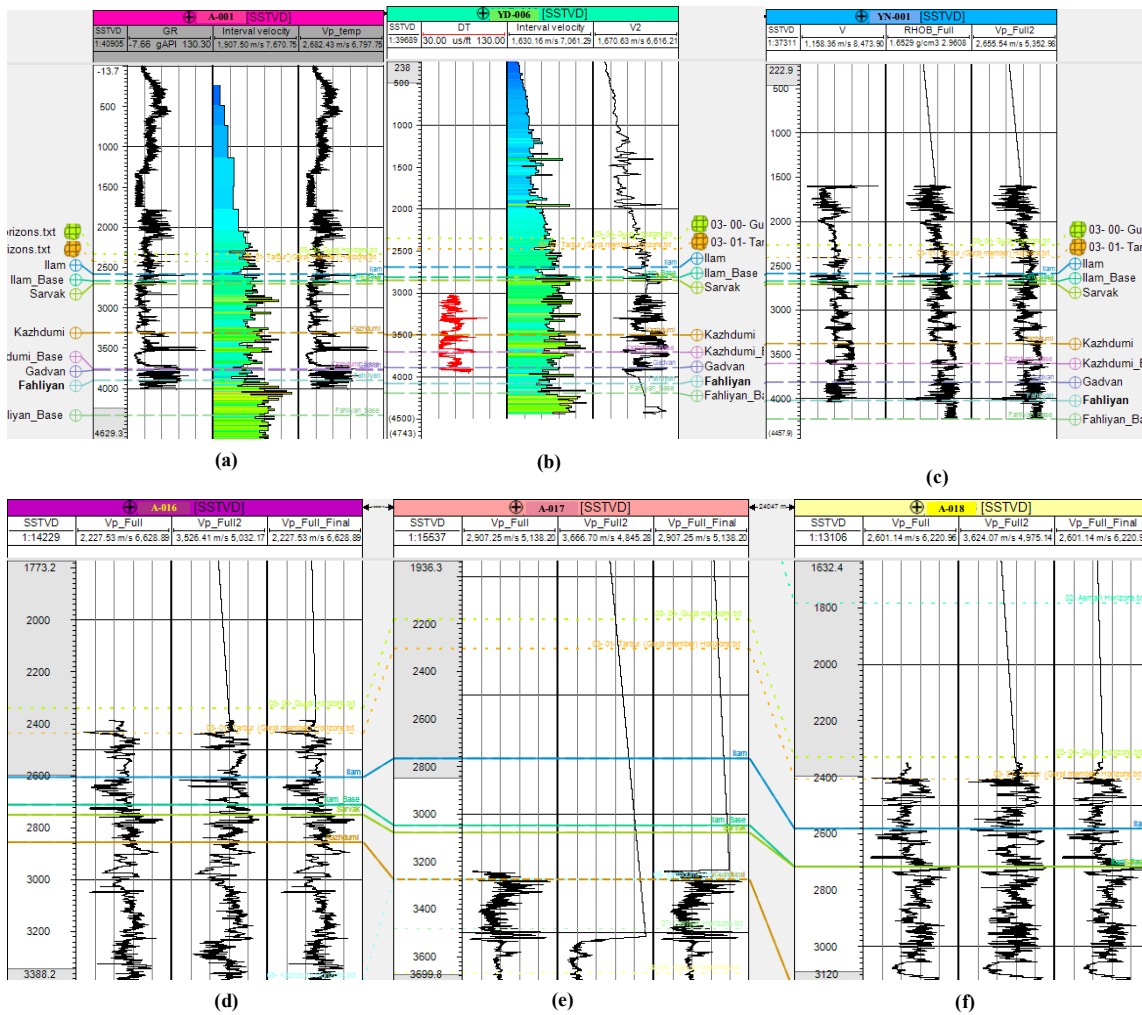


Figure 9. a) An example of primary "Vp.temp" log based on "V.VSP.int" and "Gr" log data, b) secondary "V2" log based on DT and "Vint(VSP)" log data, c) "Vp.full2" velocity log based on initial Vp log data and completed density log, d-f) examples of final "Vp.full_final" logs when "Vp.full.2" data can be used wherever "Vp.full" data is not available.

2.4. Calculate and complete shear velocity cube

Preliminary studies of shear velocity (V_s) include measuring the shear velocity from the cores of 4

exploratory wells and examining its ratio to the compressional velocity logs based on porosity and lithology changes. Each step is performed to complete the shear velocity cube and compare it

with the initial data to determine the final shear velocity cube. The DSI shear velocity (V_s) log data is discontinued in three wells. At each stage, the shear velocity cube is completed and compared with the initial data to determine the final shear velocity cube.

2.4.1. Using laboratory results of drilling cores based on porosity changes

In this section, the porosity (%) logs were scaled up as a porosity cube, and then spread in the whole studied field using a combination of the SGS

method and co-kriged with a density cube. Then based on the division of porosity data into three intervals of greater than 0.2%, between 0.1% to 0.2%, and less than 0.1% using conditional programming of Petrel 2016 software, the equation for calculating shear velocity based on compressional velocity derived from the drilling core is determined. Then after combining compressional velocity cubes using conditional programming of Petrel 2016 software, the shear velocity (V_s) cube obtained from Porosity changes is presented in Figure 10.

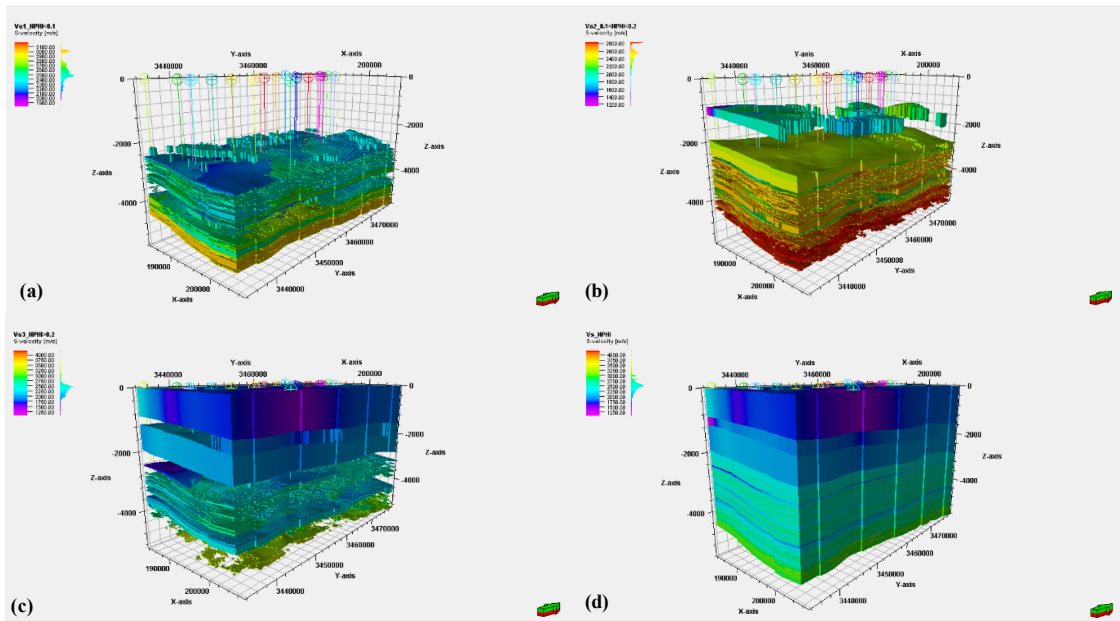


Figure 10. Shear velocity cube (m/s) based on a) porosity below 0.1% and relationship with compressional velocity and a linear correlation coefficient of 0.92, b) porosity between 0.2% to 0.1%, and relationship with compressional velocity with a non-linear correlation coefficient of 0.93, c) porosity greater than 0.2% and relationship with compressional velocity with a linear correlation coefficient of 0.97, d) combination of all shear velocity cubes.

2.4.2. Using laboratory results of drilling wells based on lithological changes

In general, if there is no shear velocity log, it is generally calculated through the relationship of Castagna (1993) using the V_p log (km/s) and lithology changes.

Limestone formation $V_s = -0.05509V_p^2 + 1.0168V_p - 1.0305$ (11)

Sandston formation $V_s = 1.0168V_p - 1.0305$ (12)

Dolomite formation $V_s = 0.583V_p - 0.07776$ (13)

Shale formation $V_s = 0.77V_p - 0.8674$ (14)

This phase of studies was made based on the relation of compressional velocity logs of four

exploratory wells and their shear velocities measured in Japan's TRC laboratory in 2002. Relations were used based on lithological changes according to the predominant lithology of sandstone, limestone, marl, and shale, as well as limestone with the highest correlation coefficients. Then by examining the lithology of all studied wells separately, the "Litho_base" shear velocity logs of each well are calculated and prepared using conditional programming of Petrel 2016 software.

For example, in one of the wells, by specifying the ranges of sandstone, limestone mixed with shale, and pure limestone based on Equation (15), the programming for construct V_s log of the well is as follows:

$$Vs = \text{If}(\text{DEPT} < 1290, (0.738 * Vp_Full_Final / 1000 - 0.5653) * 1000, \text{If}(\text{DEPT} \geq 1290 \text{ and } \text{DEPT} < 2330, (0.5243 * Vp_Full_Final / 1000 + 0.0451) * 1000, \text{If}(\text{DEPT} \geq 2330 \text{ And } \text{DEPT} < 3300, (-0.1068 * \text{Pow}(Vp_Full_Final / 1000, 2) + 1.5106 * Vp_Full_Final / 1000 - 2.2008) * 1000, \text{If}(\text{DEPT} \geq 3300 \text{ and } \text{DEPT} < 3890, (0.5243 * Vp_Full_Final / 1000 + 0.0451) * 1000, \text{If}(\text{DEPT} \geq 3890 \text{ and } \text{DEPT} < 4640, (-0.1068 * \text{Pow}(Vp_Full_Final / 1000, 2) + 1.5106 * Vp_Full_Final / 1000 - 2.2008) * 1000, U)))))) \tag{15}$$

After completing the shear velocity cubes obtained by the methods of porosity and lithology changes, the correlation coefficients of the above cubes are 0.94. It showed a high correlation between the results of the two methods, so considering that the shear velocity logs obtained from lithological changes have been calculated from well to well, the above-made logs and DSI shear velocity log have been used for data accuracy.

2.4.3. Using DSI shear velocity logs recorded in exploratory wells

The primary data records of the DSI shear velocity log included the sequence from the A-006 well in two sections of the Tarbur member of the Gurpi and Gadvan formations and the wells A-010 and A-025 in the end sections of the Gadvan until the beginning of the Lower Fahliyan. Excluding the out-of-range data, their correlation coefficient was calculated with the shear velocity data obtained from the lithology data.

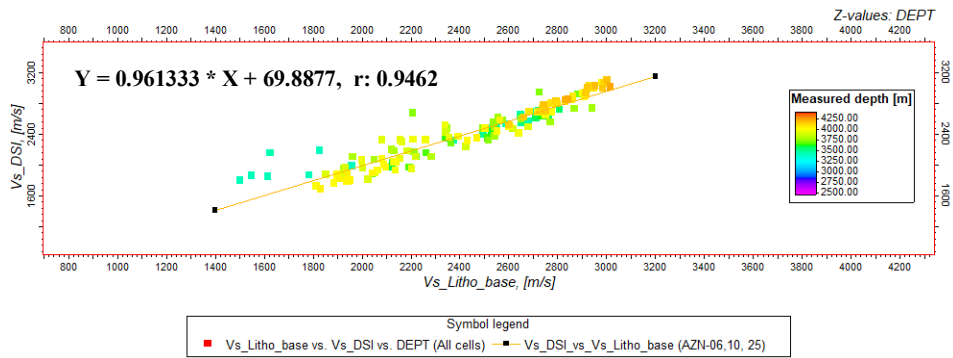


Figure 11. Relation of shear velocity resulting from lithology (“Litho_base”) compared to DSI shear velocity of three wells with information.

Based on the results, the correlation coefficient of 0.95 for the data of the shear velocity obtained from the lithology data with the main data of the DSI shear velocity showed a high accuracy of the conducted studies (Figure 11). Therefore, to prepare the final shear velocity log, the DSI shear velocity logs are replaced by the log data obtained from lithology (Figure 12). Then the final log is scaled up as a model extension to the entire cube using the inverse squared distance (IDW) method (Figures 13 and 14).

The maximum fluctuations of shear velocity are in the range of 2200 to 3000 meters per second (m/s), and the maximum is more than 3000 m/s at depths of more than 4200 meters.

In order to finally ensure the accuracy of the shear velocity model, the correlation coefficient of the final and porosity-based models was calculated at 0.95, which indicates the present model's acceptability.

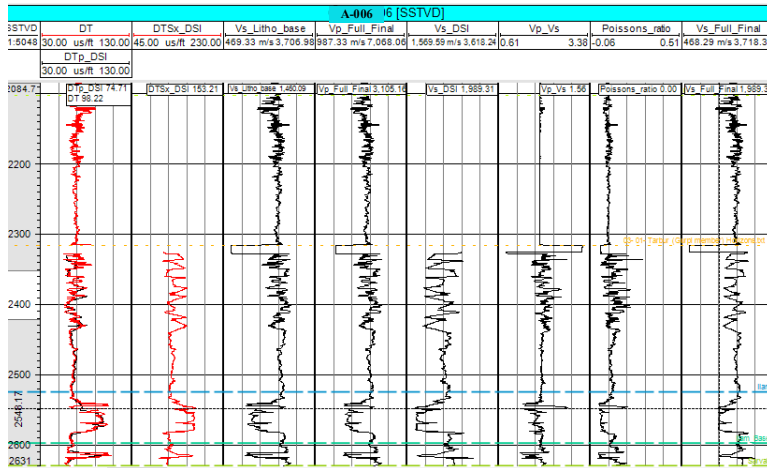


Figure 12. Final shear velocity logs after merging data of the existing DSI shear velocity and obtained from lithology data (Litho_base) of well A-006.

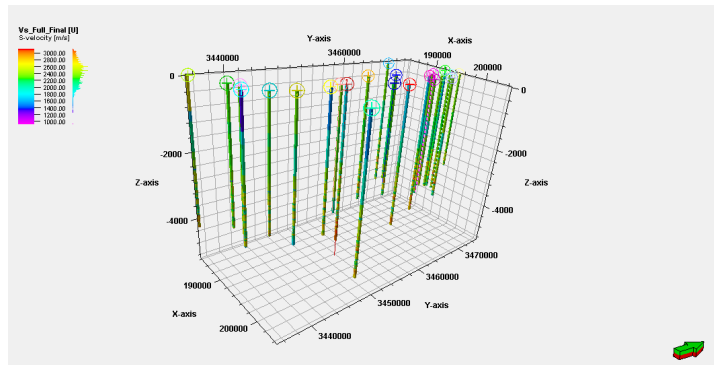


Figure 13. Scaled up Shear velocity model resulting from merging of DSI and "Litho_base" logs.

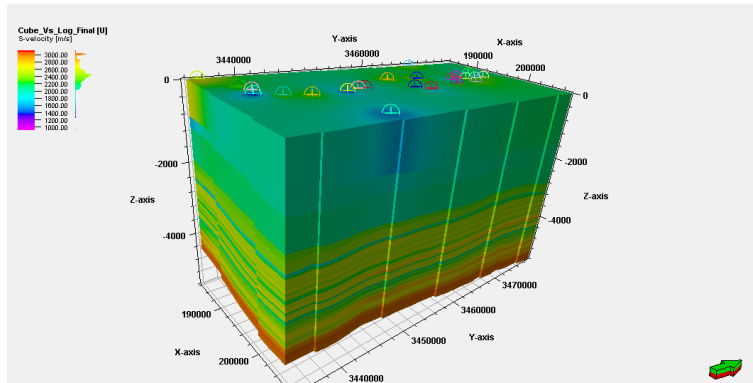


Figure 14. Final shear velocity cube (m/s) of South Azadegan field with IDW method.

2.5. Completing seismic acoustic impedance inversion (AI) and interval seismic migration velocity cubes

Generally, the seismic inversion methods are classified based on their input data and the parameter estimation methodology, which are pre-stack and post-stack inversions with deterministic or stochastic methodologies [24]. Usually, a post-stack migration scheme is applied to the seismic

data to improve the resolution by restoring dipping reflectors to their proper position. As a result, the migrated time sections are interpretable in subsurface features [25].

Pre-stack migration of noisy and low-quality data produces migrated sections of comparably lower quality than the post-stack migration of the common-reflection-surface (CRS) stack [26]. Coherent noise will be enhanced if the stack

aperture is not set appropriately, contaminating the subsequent post-stack migration section [27]. The primary post-stack seismic data and the synthetic inverted seismic data at well locations have an average correlation of 99.61% and an average

relative error of 8.76% in an acceptable range. Thus primary acoustic impedance cube with depth domain data was generated with the Hampson Russel 8 (HSR.8) software (Figure 16).

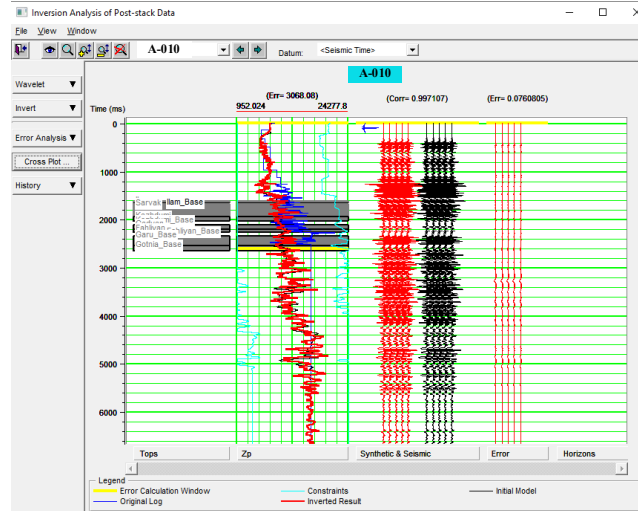


Figure 15. Sample of Analysis diagram of relative error and correlation values of inversion with post-stack data in well A-010. Uncertainty described as relative error is about 8.5%.

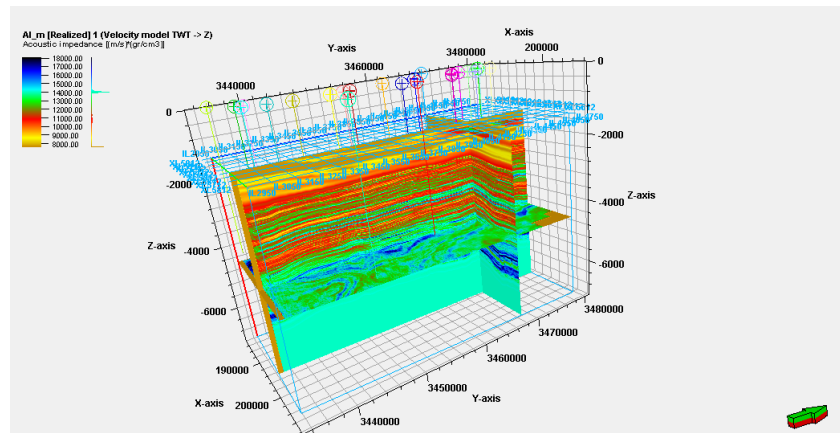


Figure 16. Converting acoustic impedance (AI) output from the Hampson Russell 8 (HSR.8) software to initial AI cube (in depth domain).

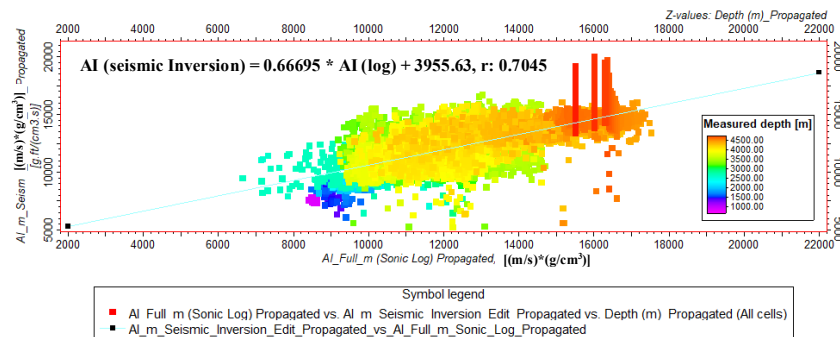


Figure 17. Determining acoustic impedance (AI) correlation coefficient from seismic inversion and log data.

The empty parts of the inverted acoustic impedance (AI) cube have been completed using the acoustic impedance cube obtained from the compressional velocity and density logs with a correlation coefficient of 0.7 (Figures 17 and 18). Based on the results obtained, the final values of inverted acoustic impedance at low depths are mostly in the range of 8000-15000 [(m/s)*(g/cm³)],

which can be in the range of calcareous formations. The Aghajari surface formation with a value of less than 8000 [(m/s)*(g/cm³)] is located in the Marley and shale formations, the results of which are highly consistent with the geological samples during drilling. The highest acoustic impedance values are in the field's lower part in the range of the lower Fahliyan formations to Gotnia.

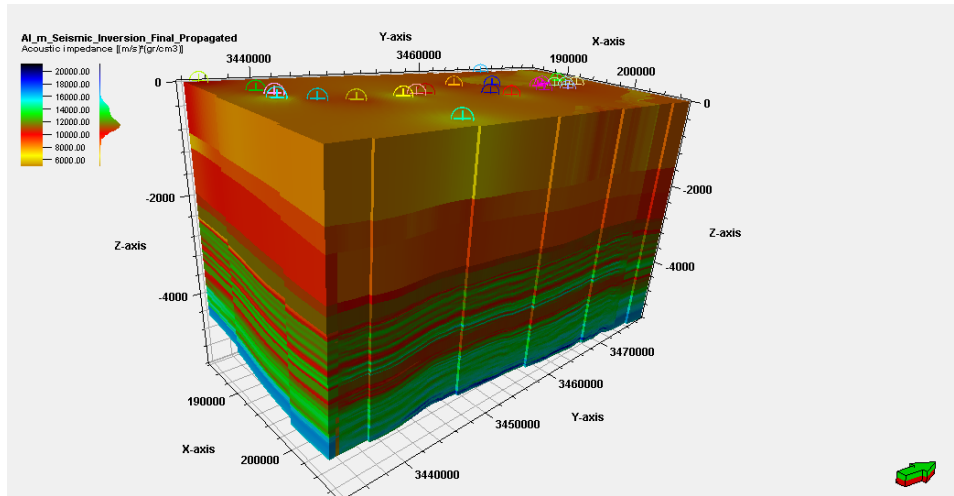


Figure 18. Final AI cube resulting from seismic inversion and log data integration.

After entering the post-stack seismic data and constructing the relevant petro-physical model, a seismic migration velocity cube was constructed

(Figure 19). The AI and interval migration cubes were used to select the final velocity model.

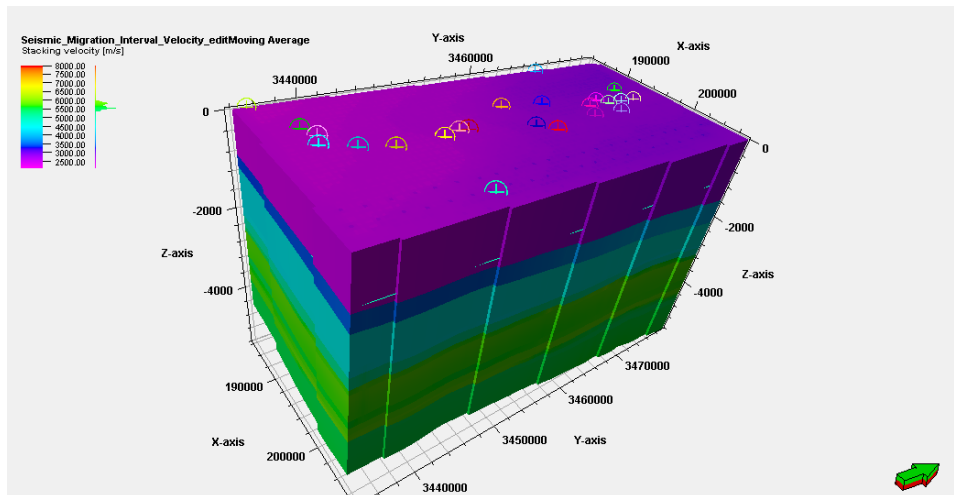


Figure 19. Interval migration velocity cube based on seismic post-stack data.

3. Results and discussion

3.1. Determining secondary velocity model by combining SGS and co-kriging methods

For determining the final velocity model, the completed data of compressional velocity (V_p) logs is re-modeled using a sequential Gaussian

simulation (SGS) combined co-kriging with acoustic impedance inversion cubes as seismic migration velocity cubes separately. Both have been re-modeled after calculating the correlation coefficients of their cubes with the initial V_p cube modeled with the IDW method (Figures 20 and 21).

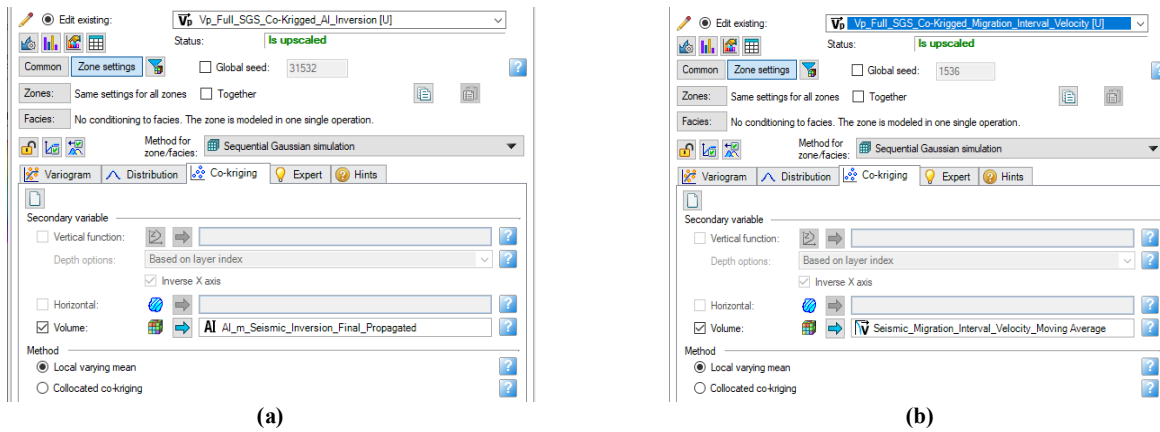


Figure 20. Method of constructing secondary compressional velocity cube (V_p) using SGS method combined with co-kriging with a) acoustic impedance cube (AI) resulting from seismic inversion and b) seismic interval migration velocity cube.

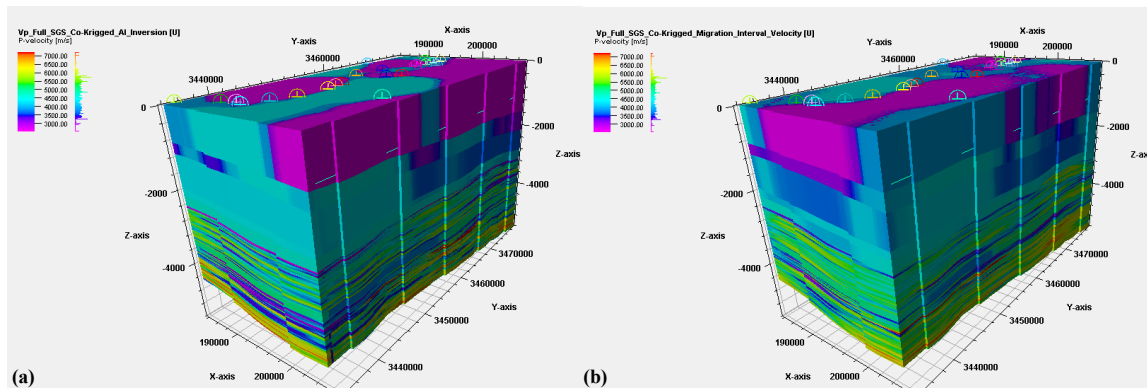


Figure 21. Secondary compressional velocity cube by SGS method and co-kringed with a) acoustic impedance (AI) cube resulting from seismic inversion, b) interval seismic migration velocity cube.

As a result, the correlation coefficient of compressional velocity cube (V_p) resulting from SGS (combined with co-kriging method with the AI inverse seismic cube) and the initial velocity cube using the inverse distance weighted (IDW) method is 0.54 (Figure 22.a), as well as the correlation coefficient of the V_p cube resulting from SGS (combined with co-kriging with the interval seismic velocity cube) and the initial velocity cube using the IDW method is 0.51 (Figure 22.b). Therefore, to model the effective pressure using the Bowers method, it is recommended to use the compressional velocity cube obtained from SGS combined with co-kriging with seismic acoustic impedance (AI) cube method.

3.2. Anisotropic spatial variation of final compressional velocity cube

For evaluating anisotropy variations in the final V_p cube (combined SGS and co-kringed with AI) model, experimental variograms with the Gaussian method were created in three directions: vertical, major horizontal azimuth of zero degrees, and the minor azimuth of 270 degrees. In the vertical Variogram, the sill is 0.34, and in major and minor is 0.96. Anisotropy range based on Petrel 2016 software computations for vertical variogram range is 96, and for major and minor directions, is 11850 meters. The experimental calculations and anisotropy range are shown in Tables 3 and 4, also semi-variograms are shown in Figures 23 and 24.

Table 3. Experimental Variogram computation for final velocity cubes.

Direction	Azimuth	Dip	Number of lags	Lag distance	Search radius	Band width	Tolerance angle	Lag tolerance	Thickness
Vertical	NA	90	8	25	200	50	45	50	0.001
Major	0	0	8	250	2000	200	45	50	0.001
Minor	270	0	8	250	2000	200	45	50	0.001

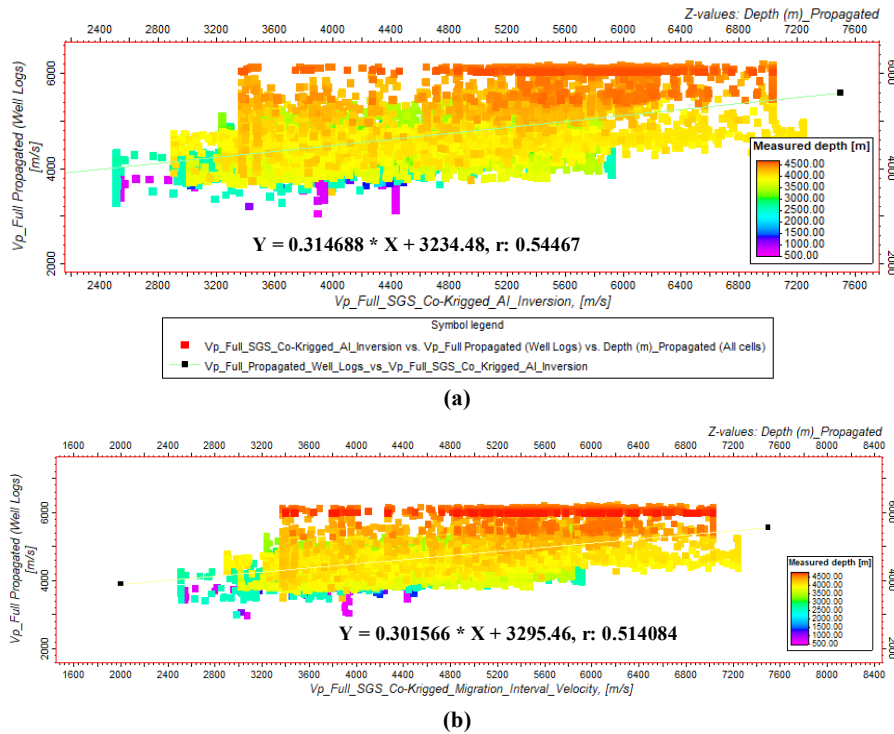


Figure 22. a) Correlation coefficient of V_{p1} cube (resulting from combined SGS and co-kriged with AI cube) and initial velocity cube with IDW method, b) Correlation coefficient of V_{p2} cube (resulting from SGS and co-kriged with migration velocity cube method) and initial velocity cube with IDW method in the south Azadegan field.

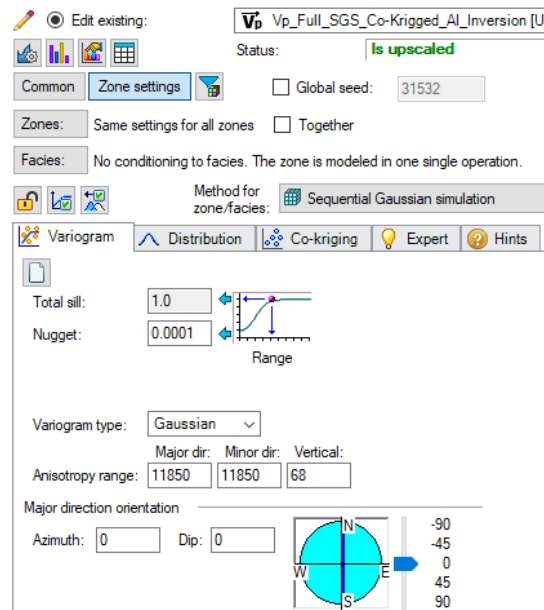


Figure 23. Anisotropy range (m) and major direction of final V_p cube variogram.

Table 4. Results of Gaussian Variogram of compressive velocity cube obtained by combining SGS and Co-kriging methods with acoustic impedance (AI) in studied field.

Direction	Nugget	Sill	Range	Number of Pairs	Anisotropy range (m)
Vertical	0.659	0.341	1000	13374251	Vertical: 68
Major azimuth 0	0.0351	0.965	7766.6	11367363	Major direction:11850
Minor azimuth 270	0.0341	0.966	7611.4	11058663	Minor direction:11850

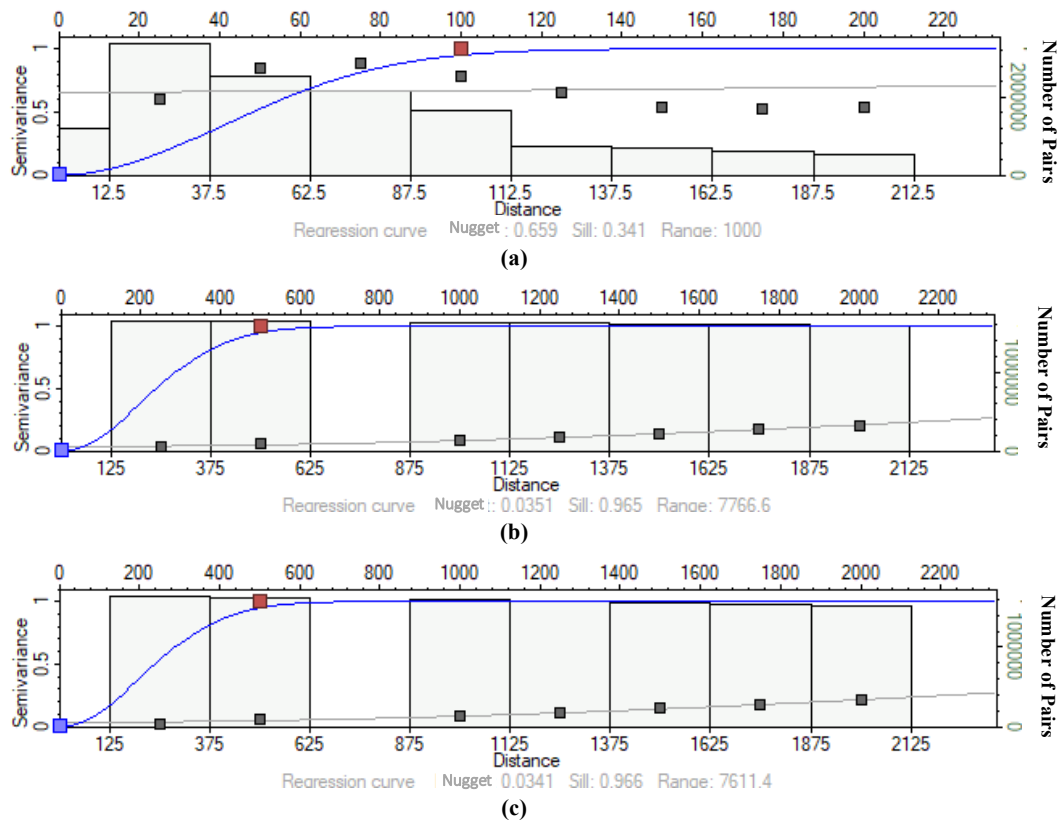


Figure 24. Semi-variogram of final V_p Cube a) Vertical, b) horizontal major direction azimuth zero deg., c) minor direction azimuth 270 deg.

3.3. Uncertainty analysis of final compressional velocity (V_p) model

In order to analyze the uncertainty of the final compressional velocity (V_p) model, the blind well test method was used. In this method, one or some of the wells with complete information in different parts of the studied field is removed at each stage. The remained V_p logs have scaled up. A new V_p model was generated like the final model using Sequential Gaussian Simulation (SGS) and co-kriged with the acoustic impedance (AI) inversion cube. Then another V_p model with the well

removed in the previous step was prepared, and their correlation diagram was calculated. The studies were carried out in several stages separately. An uncertainty analysis example is removing three indicator wells in the southwest and center of the field including A-006, A-010, and A-025 wells with a final uncertainty coefficient of 0.43, which are presented in Figures 25 and 26. In general, the amount of correlation obtained from uncertainty studies is about 50%, which is acceptable considering the large number of 23 exploratory and production wells (Table 5).

Table 5. Uncertainty analysis of final V_p model with removing some indicator wells and using SGS method combined with co-kriging with seismic acoustic impedance inversion cube (AI) in studied field.

Row	Used well for 1st propagated V_p cube	Used well for 2nd propagated V_p cube	Correlation coefficient of propagated V_p models
1	All except A-001	Only A-001	0.421355
2	All except A-006	Only A-006	0.38445
3	All except A-010	Only A-010	0.42301
4	All except A-025	Only A-025	0.551237
5	All except A-006, A-010, and A-025	Only A-006, A-010, and A-025	0.43123
6	All except YD-006	Only YD-006	0.506639

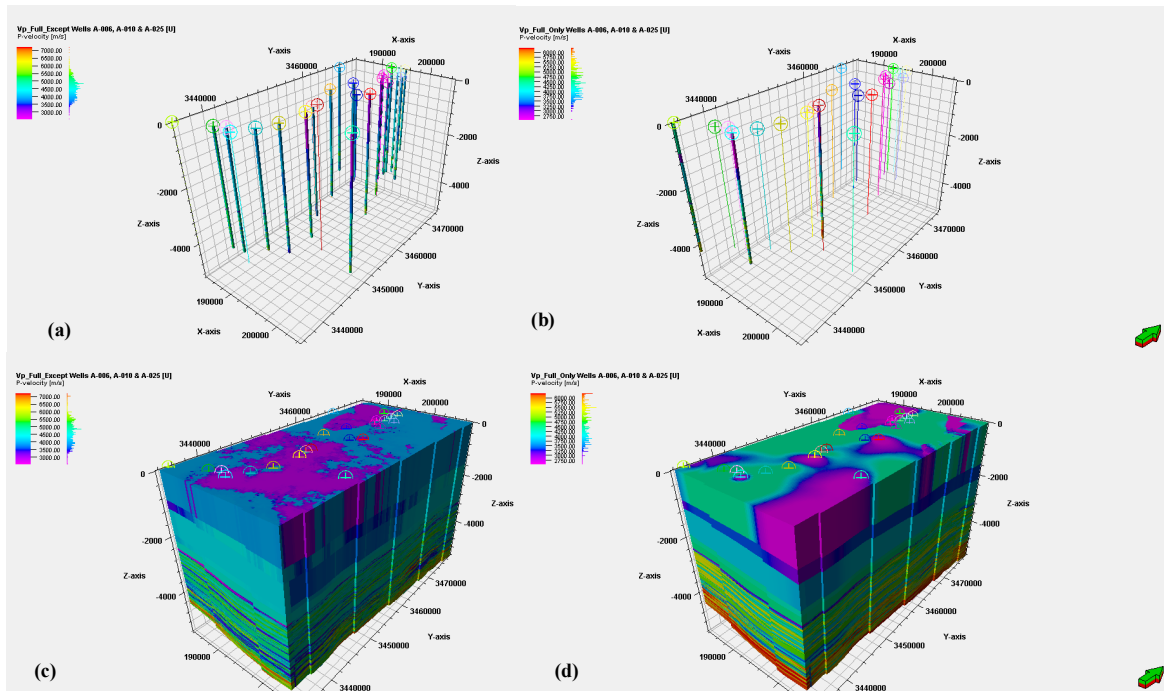


Figure 25. Uncertainty analysis with a) all scaled up Vp logs except A-006, A-010 and A-025 wells, b) scaled up only with A-006, A-010, and A-025 wells, c) propagating Vp cube with all scaled up logs except A-006, A-010, and A-025 wells, d) propagated Vp cube only with scaled up A-006, A-010, and A-025 wells

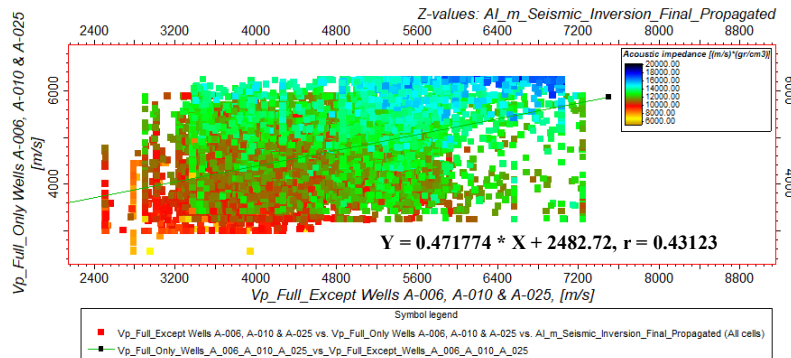


Figure 26. Uncertainty analysis of propagated Vp cubes with calculating correlation coefficient of cubes except three indicator wells and only with these three wells in studied field.

3.4. Fractal model of compressional velocity-volume (Vp-V)

After completing the modeling of the final compressional velocity cube data of the South Azadegan field, due to the high volume of data rows of about 1.5 million (every 15 cm depth change, one data cube cell), intervals of 1000 meters were analyzed. The results will be presented as velocity-volume (Vp-V) models based on Equation (16).

$$V(\geq V_p) \propto V_p^{-\beta} \tag{16}$$

In this relation, V includes the larger and equal compressional velocity (Vp) sample volume, and β is the fractal dimension.

Division of South Azadegan field based on the average cubic thickness of geological layers using the Petrel 2016 software shown in Table 6. Based on the average thickness divisions of the geological models, each of the Aghajari, Asmari, Pabdeh, Sarvak, Khalij member, and Sargelu formations are located in the common parts of the two intervals of fractal models. Thus each model calculates the number of its data cells separately.

The fractal value-volume diagrams obtained from the cube of compressional velocity (Vp) were prepared for depths of 1000 meters. In the interval

from surface to 1000 meters, there are seven regimes of compressional velocity between less than 3357.4 and 4405.5 m/s in the Aghajari formation. In Continuing up to 2000 meters, two V_p regimes between 3162.28 and 3801.9 m/s are observed in the continuation of Aghajari and Gachsaran formations, and two other V_p regimes between 4265.8 and more than 4385.3 m/s, which can represent the Asmari and Pabdeh formations. In the depth of 2000 to 3000 meters, four regimes resulting from the three breaking points of the diagram between 3890.4 and 5011.9 m/s can be observed between the Asmari and Sarvak formations. In the distance of 3000 to 4000 meters, there are four regimes resulting from three

breaking points between 4466.8 and 5754.4 m/s in the distance from Kazhdumi to Khalij member of Gadvan formation. In the depth of 4000-5000 meters, eight regimes between 4415.7 and 6237.4 m/s are observed between the Khalij member of Gadvan and a part of Sargelu formations. Finally, in depths 5000 to 5590 meters, there are four compressional velocity regimes with three breaking points between 5956.6 and 6109.4 m/s corresponding to the Najmeh to Neyriz formations in the Jurassic period. All fractal model graphs of value-volume intervals of surface-5590m cubic meters pressure velocity of the South Azadegan field are presented in Figure 27 (a-f).

Table 6. Division of South Azadegan field based on average cubic thickness of geological layers (using Petrel 2016 software).

Row	Formation	Formation top (m)	Formation base (m)	Average thickness (m)	Dominant lithology	Number of data cubes
1	Aghajari	0	1272.3	1272.3	Marl and sandstone	14,090
2	Gachsaran	1272.3	1630.65	358.35	Anhydrite and Claystone	7,571
3	Asmari	1630.65	2368.25	737.6	Sandstone and Limestone	17,579
4	Gurpi	2368.25	2590.05	221.8	Limestone	26,650
5	Tarbur (Member)	2590.05	2757.85	167.8	Limestone and marl	93,179
6	Ilam and Laffan	2757.85	2866.05	108.2	Limestone and claystone	64,678
7	Sarvak	2866.05	3506.9	640.85	Limestone	382,420
8	Kazhdumi	3506.9	3733.95	227.05	Shale, Limestone and Sandstone	150,607
9	Dariyan	3733.95	3896	162.05	Limestone and marl	134,788
10	Gadvan	3896	3966.55	70.55	Marl, shale and limestone	85,320
11	Khalij (member)	3966.55	4071	104.45	Sandstone and Limestone	139,131
12	Upper Fahliyan	4071	4228.05	157.05	Limestone	190,818
13	Lower Fahliyan	4228.05	4589.1	361.05	Limestone	199,299
14	Garau	4589.1	4783	193.9	Limestone and claystone	75,612
15	Gotnia	4783	4931	148	Anhydrite and limestone	45,221
16	Najmeh	4931	4959	28	Anhydrite and limestone	6,678
17	Sargelu	4959	5068	109	Limestone and shale	17,858
18	Alan	5068	5107	39	Anhydrite and limestone	3,900
19	Muss	5107	5199	92	Limestone	7,089
20	Neyriz	5199	5590	391	Limestone and anhydrite	7,873

3.5. Correlation of compressional velocity and geological models by Logratio matrix

The compressional velocity-volume (V_p - V) fractal diagrams were constructed for each 1000 meter. Then the breaking points of each compressional velocity interval are determined as a mathematical model. Then based on changes in the formation and lithology of the above intervals (geological model), the Logratio matrix has calculated to determine the highest compliance and lowest error. Calculating the Logratio matrix for 0-1000 m interval has been omitted due to the small changes in this interval's lithology, mostly marl and sandstone.

Based on the division of V_p regimes in depths of 1000 to 5590 meters into 25 different regimes and determining the dominant geological model of

each regime (including 20 ranges of pure limestone, three ranges of sandstone and limestone, one range of anhydrite and sandstone, and one interval of marl and sandstone), logarithmic matrices are calculated separately (An example shown in Table 7).

According to Table 8, in the dominant limestone intervals, the highest overall accuracy (OA) of 0.74 in the compressional velocity range of fewer than 6109.4 m/s at depths of 5000-5590 meters is related to Najmeh to Neyriz formations. Moreover, the lowest rate of 0.32 in the compressional velocity range between 6011.7 to 6095.4 m/s is related to the Khalij member of Gadvan formation to Sargelu at depths of 4000-5000 meters. In sandstone and limestone domains, the highest overall accuracy is 0.64 in the compressional velocity range between

1801.9 to 4265.8 m/s at depths of 1000-2000 meters related to Aghajari to Pabdeh formations. Therefore, according to the predominant calcareous intervals, the maximum OA is calculated to be 0.74, which indicates the high

correlation of the compressional velocity cube model obtained by sequential Gaussian simulation (SGS) with co-kriging with acoustic impedance (AI) inversion.

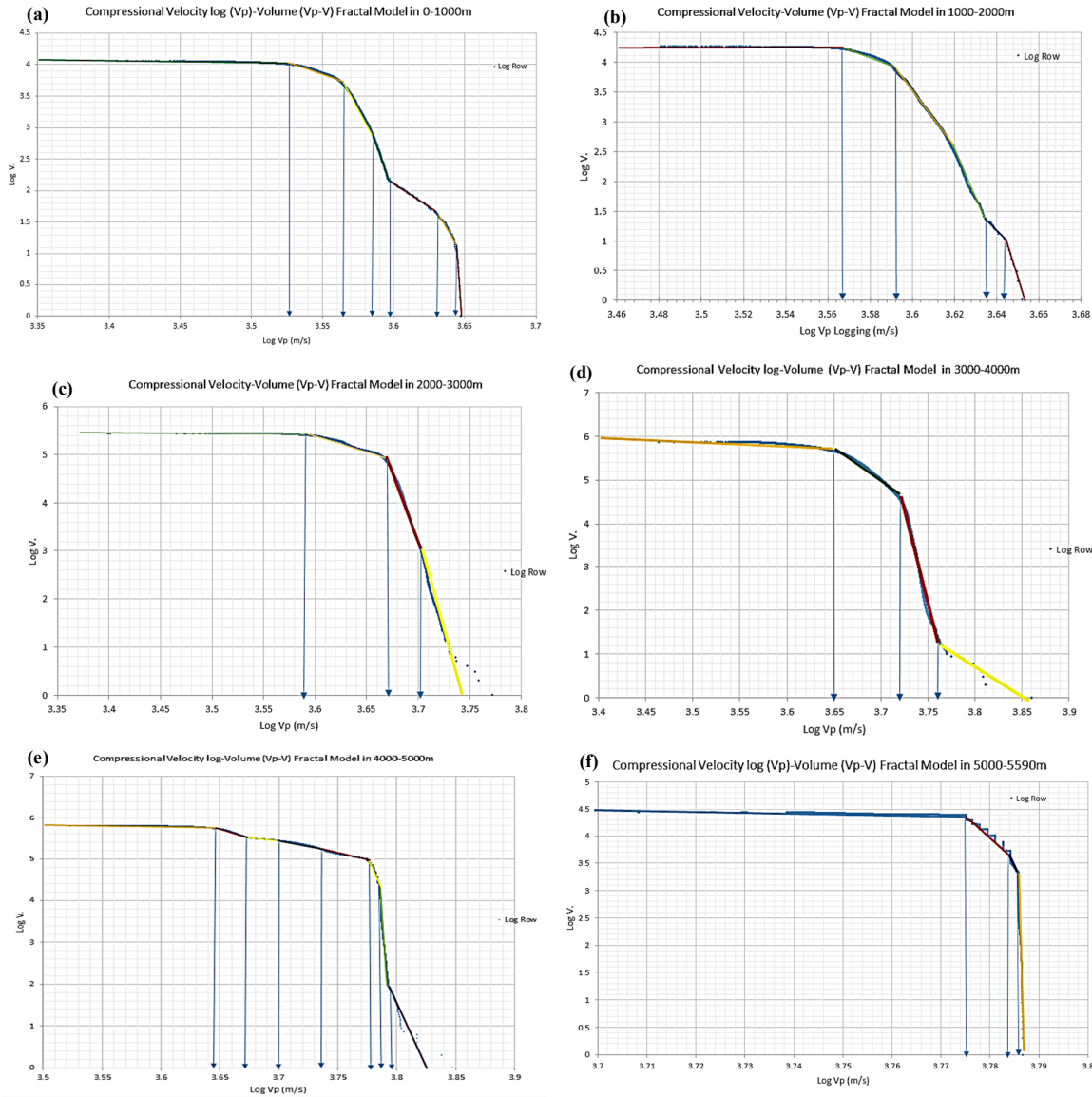


Figure 27. Fractal model of compressional velocity-volume (Vp-V) a) surface-1000 m (Aghajari formation), b) 1000-2000m (Aghajari to Pabdeh formations), c) 2000-3000 m (Pabdeh to upper of Sarvak formations), d) 3000-4000 m (Sarvak to Khalij member of Gadvan formations), e) 4000-5000m (Khalij to Sargelu formations), and f) 5000-5590 m (Najmeh and Sargelu to Neyriz formations).

Table 7. Logratio matrix mathematical model of V_p between 4466.8 to 5248.1 m/s and geological model of dominant limestone distance 3000-4000 meters.

Mathematical Model (V_p : 4466.8-5248.1 m/s)	Geological model (dominant limestone)				
		Inside zone		Outside zone	
		Inside zone	Outside zone		
	Inside zone	True positive (A)	235343	False positive (B)	186789
	Outside zone	False negative (C)	73439	True Negative (D)	225686
		Type I error: C/(A+C)	0.2378	Type II error: B/(B+D)	0.4530
		Overall accuracy: (A+D)/(A+B+C+D)			0.6391

Table 8. Total error values and overall accuracy (OA) of logratio matrices of compressional velocity mathematical models and dominant geological models in south Azadegan field.

Interval (m) and formation	Compressional velocity regimes	Mathematical model (Vp (m/s))	Geological model (dominant lithology)	Mathematical analysis (Type I error)	Geological sampling (type II error)	Overall accuracy (OA)
1000-2000 Aghajari, Gachsaran, Asmari, and Pabdeh	5	< 3162.3	Marl and sandstone	0.988	0.000	0.85
		3162.3-3801.9	sandstone and Limestone	0.921	0.436	0.36
		3801.9-4265.8	sandstone and Limestone	0.081	0.557	0.64
		4265.8-4385.3	sandstone and Limestone	0.998	0.002	0.58
		> 4385.3	Anhydrite and Claystone	0.998	0.000	0.57
2000-3000 Asmari, Pabdeh, Gurpi, Ilam, and Sarvak	4	< 3890.4	Limestone	0.935	0.070	0.61
		3890.4-4677.4	Limestone	0.405	0.711	0.40
		4677.4-5011.9	Limestone	0.672	0.216	0.61
		> 5011.9	Limestone	0.988	0.003	0.63
3000-4000 Kazhdumi, Dariyan, Gadvan, and Khalij member	4	< 4466.8	Limestone	0.806	0.488	0.38
		4466.8-5248.1	Limestone	0.238	0.453	0.64
		5248.1-5754.4	Limestone	0.956	0.059	0.56
		> 5754.4	Limestone	1.000	0.000	0.57
4000-5000 Khalij member of Gadvan, Fahliyan, Garau, Gotnia, Najmeh, and Sargelu	8	< 4415.7	Limestone	0.851	0.142	0.41
		4415.7-4677.4	Limestone	0.630	0.182	0.54
		4677.4-5011.9	Limestone	0.848	0.076	0.44
		5011.9-5432.5	Limestone	0.818	0.101	0.45
		5432.5-6011.7	Limestone	0.892	0.264	0.34
		6011.7-6095.4	Limestone	0.984	0.164	0.32
		6095.4-6237.4	Limestone	0.977	0.071	0.36
		> 6237.4	Limestone	1.000	0.000	0.37
5000-5590 Najmeh, Sargelu, Alan, Muss, and Neyriz	4	< 5956.6	Limestone	0.917	0.139	0.67
		5956.6-6081.35	Limestone	0.327	0.694	0.40
		6081.35-6109.4	Limestone	0.758	0.158	0.69
		> 6109.4	Limestone	0.998	0.009	0.74

4. Conclusions

1. According to the interval velocity model, the highest average velocity in the range of 2760-2900 m/s in the northeast of the study area is related to the Gotnia formation, and the lowest is related to the Gachsaran formation with 2150-2280 m/s in the southwest direction of the case study area.
2. Due to the lack of surface compressional velocity logs data in no one of the wells, using artificial neural networks to construct velocity models in surface layers was impossible. Thus using VSP, gamma rays and density logs were done in 5 steps with the highest possible correlation coefficient, and a scaled-up model was constructed for all wells from surface to bottom.
3. In order to study the fracture pressure of the formation, the shear velocity cube was modeled using exploratory well cores and shear velocity logs. The final Vs logs had a 0.95 correlation with the main DSI shear logs.
4. Cube values of inverted acoustic impedance in the depths of the bottom of the field are often in the range of 8000-15000 [(m/s)*(g/cm³)], which can be in the range of calcareous formations.
5. Aghajari surface formation with acoustic impedance (AI) of less than 8000 [(m/s)*(g/cm³)] is located in Marley and shale formations, the results of which are highly consistent with geological samples during drilling.

6. In order to model the effective pressure using the Bowers method, it is recommended to use the compressional velocity cube obtained from SGS combined with co-kriging with seismic acoustic impedance (AI) cube method. As a result, the correlation coefficient of the V_p cube resulting from SGS (combined with co-kriging method with the AI inverse seismic cube) and the initial velocity cube using the inverse distance weighted (IDW) method is 0.54, as well as the correlation coefficient of the V_p cube resulting from SGS (combined with co-kriging with the interval seismic velocity cube) and the initial velocity cube using the IDW method is 0.51.

7. In the Final V_p cube's vertical Variogram, the sill is 0.34, and in major and minor is 0.96. Anisotropy range for vertical variogram range is 96 meter and for major and minor directions is 11850 meters.

8. In general, the amount of correlation obtained from uncertainty studies of Vp model is about 50%, which is acceptable considering the large number of 23 exploratory and production wells.

9. Based on the velocity-volume (Vp-V) fractal models, compressional velocity regimes are divided into 25 regimes at distances of 1000 to 5590 meters. The dominant geological model of each regime includes 20 intervals of pure limestone, three intervals of sandstone and limestone, one interval of anhydrite and sandstone, and one interval of marl and sandstone.

10. Based on the results of the Logratio matrix in the dominant limestone intervals, the maximum overall accuracy (OA) of 0.74 in the V_p range of fewer than 6109.4 m/s at depths of 5000-5590 meters is related to the Najmeh to Neyriz formations. Also the lowest OA of 0.32 in the V_p range of 6011.7-6095.4 m/s is related to the Khalij member of Gadvan to Sargelu formations at depths of 4000-5000 meters.

Nomenclatures

AI:	Acoustic impedance [(m/s)*(g/cm ³)]
ANN:	Artificial neural network
DT:	Delta T Sonic Transit Time (us/ft.)
DSI:	Dipole sonic imager
DST:	Drill stem test
MDT:	Modular dynamic tester
IDW:	Inverse distance weighted
OA:	Overall accuracy
r:	Correlation coefficient
RFT:	Repeat formation test
SGS:	Sequential gaussian simulation
TWT:	Two wave travel time (m.s)
SW:	Southwest
V_{avg}:	Average velocity (m/s)
V_{int}:	Interval velocity (m/s)
VP:	Compressional velocity (m/s)
Vs:	Shear velocity (m/s)
VSP:	Vertical seismic profiling

Acknowledgment

The present work is from a PhD dissertation on Mining Engineering-Mineral Exploration from Islamic Azad University, South Tehran Branch, hosted by the Research Institute of Petroleum Industry (RIPI). The authors consider it necessary to express their sincere gratitude to the esteemed experts of the RIPI and Exploration Directorates of the National Iranian Oil Company (NIOC). They helped us to carry out and improve the quality of this research.

References

- [1] Maddahi, A., Ghazi Nezhad, S., Ismailpour, S., and Heydari, M. (2014). Feasibility study of exploiting four-dimensional seismic studies of Sarvak reservoir in Azadegan field, Journal of Petroleum Research, No. 78, p. 126-117 (in Persian).
- [2] Adim, A., Riahi, M., and Bagheri, M. (2018). Estimation of pore pressure by Eaton and Bowers methods using seismic and well survey data, Journal of Applied Geophysical Research, Volume 4, Number 2, p. 275-267, Digital Identification (DOI): 10.22044 / JRAG.2018.6360.1167 (in Persian).
- [3] Poorsiami, H. (2013). Modeling the pore pressure of a hydrocarbon reservoir in southwestern Iran using well-

logging data, Journal of Petroleum Research, Volume 23, Number 74, p. 86-72 (in Persian).

[4] Aghebati, R. (2008). Introduction of a field: Azadegan field development plan, scientific Journal of Oil and Gas exploration and production, number 51, November 2008 p. 8-6 (in Persian).

[5] Jindal N., Kumar Biswal A., and Hemant Singh K. (2016). Time-Depth Modeling in High Pore-Pressure Environment, Offshore East Coast of India, AAPG 2016 Annual Convention and Exhibition, Calgary, Alberta, Canada, June 19-22, 2016.

[6] Haris A., Sitorus R.J., and Riyanto A. (2017). Pore pressure prediction using probabilistic neural network: case study of South Sumatra Basin, Southeast Asian Conference on Geophysics, IOP Conf. Series: Earth and Environmental Science 1 26324 (526071879)0 012021.

[7] Amirzadeh, M., Kamali, M.R., and Nabi Bidehandi, M. (2013). Investigation of reservoir characteristics by performing seismic data conversion and seismic markers in Sarvak Formation in one of the oil fields in southwestern Iran, Journal of Petroleum Research, Vol. 23, No. 75, 2013, p. 29-20 (in Persian).

[8] Amiri Bakhtiar, M.S., Zargar, Gh, Riahi, M.A., and Ansari, H.R. (2017). Seismic inversion by spectral simulation in one of the oil fields in southwestern Iran, the third oil exploration geophysics seminar, Exploration Directorate of the National Iranian Oil Company, May 2017, pp. 74-70 (in Persian).

[9] Castagna J. P., Batzle M. L., and Eastwood R. L (1985) Relationships between compressional-wave and shear-wave velocities in clastic silicate rocks, GEOPHYSICS, VOL. 50, NO.4 (APRIL 1985); P. 571-581, 25 FIGURES, 2 TABLES.

[10] Castagna, J. P., Batzle, M.L. and Kan, (1993). Rock Physics: The link between rock properties and AVO response, In: Offset-dependent reflectivity - Theory and practice of AVO analysis, Castagna, J.P. and Backus, M. M., editors. Investigations in Geophysics no. 8, SEG, OK, 135-171.

[11] Fatahi, H., Askari, M., Majdi and Far, S. (2016). Estimation of shear wave velocity in one of the hydrocarbon reservoirs of southwest Iran using different well logs and a new intelligent combined method Journal of Advanced Applied Geology, Winter 95, No. 22. pp. 35-43 (in Persian).

[12] Bowers, G. (1995). Pore Pressure Estimation from Velocity Data: Accounting for Overpressure Mechanisms Besides Undercompaction, SPE Drilling & Completion, Vol. 10, No. 2, p. 89-95, 1995.

[13] Bowers G.L. (2002). Detecting high overpressure, The Leading edge, 21 (2) (2002), pp. 174-177.

[14] Lantuejoul, C.h. (2002). Geostatistical Simulation Models and Algorithms, Springer-Verlag Berlin Heidelberg GmbH, ISBN: 978-3-662-04808-5, 256 p.

- [15] Kelkar, M. and Perez, G. (2002). Applied Geostatistics for Reservoir Characterization, Society of Petroleum Engineers. ISBN: 978-1-55563-095-9, 264 p.
- [16] Bohling, G. (2007). INTRODUCTION TO GEOSTATISTICS, Hydro-geophysics: Theory, Methods, and Modeling, Boise State University, Boise, Idaho.
- [17] Armstrong, M., Galli, A., Beucher, H., LeLoc'h, G., Renard, D., Eschard, R., Doligez, B., and Geffroy, F. (2011). Pluri-gaussian Simulations in Geosciences, Springer-Verlag Berlin Heidelberg GmbH, ISBN: 978-3-662-12718-6, Pages: 149.
- [18] Hassanpour, S., and Afzal, P. (2013). Application of concentration–number (C–N) multifractal modeling for geochemical anomaly separation in Haftcheshmeh porphyry system, NW Iran. Arab J Geosci **6**, 957–970.
- [19] Paravarzar, S., Maarefvand, P., Maghsoudi, and A. Afzal, P. (2014). Correlation between geological units and mineralized zones using fractal modeling in Zarshuran gold deposit (NW Iran). Arab J Geosci **8**, 3845–3854.
- [20] Soltani, F., Afzal, P., and Asghari, O. (2014). Delineation of alteration zones based on Sequential Gaussian Simulation and concentration–volume fractal modeling in the hypogene zone of Sungun copper deposit, NW Iran. Journal of Geochemical Exploration, **140**, 64–76. doi: 10.1016/j.gexplo.2014.02.007
- [21] Carranza EJM (2011). Analysis and mapping of geochemical anomalies using logratio-transformed stream sediment data with censored values. J Geochem Explor **110**(2):167–185.
- [22] Mokhtari M, Zandifar H, and Abdollahie Fard I (1999). Seismic Interpretation of top Sarvak Formation in Azadegan-Nir Kabir Area (SW Iran), National Iranian Oil Company, Exploration Directorate, Published report in Farsi.
- [23] Abdollahie Fard I (2006) Structural models for the South Khuzestan area based on reflection seismic data, Ph.D. Dissertation in Geology Tectonics, School of Earth Sciences, Shahid Beheshti University, Tehran, Iran
- [24] Shahbazi, A., Soleimani Monfared, M., Thiruchelvam, V., Ka Fei, T., and Babasafari, A.A. (2020). Integration of knowledge-based seismic inversion and sedimentological investigations for heterogeneous reservoir. Journal of Asian Earth Sciences, **202**, 104541.
- [25] Rointan, A., Soleimani Monfared, M. and Aghajani, H. (2021). Improvement of seismic velocity model by selective removal of irrelevant velocity variations. Acta Geodaetica et Geophysica **56**, 145–176.
- [26] Soleimani, M. (2016). Seismic imaging by 3D partial CDS method in complex media. Journal of Petroleum Science and Engineering, **143**.
- [27] Shahbazi, A. Ghosh, D., Soleimani, M., and Gerami, A. (2016), Seismic imaging of complex structures with the CO-CDS stack method. Studia Geophysica et Geodaetica. **60**, 662–678.

مدلسازی سرعت های فشاری و برشی لایه ای به منظور تعیین فشارهای سازندی در یکی از میداین جنوب غرب ایران

پوریا کیانوش^۱، قدرت اله محمدی^{۱*}، سید علی اکبر حسینی^۲، ناصر کشاورز فرج خواه^۳، پیمان افضل^۱

۱- گروه مهندسی نفت و معدن، دانشگاه آزاد اسلامی، واحد تهران جنوب، تهران، ایران

۲ - گروه مهندسی نفت، مواد و معدن، دانشگاه آزاد اسلامی، واحد تهران مرکز، تهران، ایران

۳- گروه پژوهش ژئوفیزیک، عضو هیئت علمی پژوهشکده علوم زمین، پژوهشگاه صنعت نفت، تهران، ایران

ارسال ۲۰۲۲/۰۷/۰۲، پذیرش ۲۰۲۲/۰۸/۱۱

* نویسنده مسئول مکاتبات: ghodrattollah46@gmail.com

چکیده:

در روش های لرزه ای، تخمین فشار های سازندی با تبدیل سرعت لرزه ای به فشار منغذی و همسان سازی آن با نگار سرعت و کالیبراسیون نتایج با فشار موثر حاصل از آزمایش چاه بدست می آید. این مطالعه چالش جدیدی در زمینه مطالعات سرعت در یکی از میداین دشت آبادان واقع در جنوب غربی ایران است که سازندهای هدف عموماً کربناته بوده و بجز سازند کزده می فاقد میان لایه های شیل هستند، فراهم می سازد. این تحقیق بر اساس داده های ۲۳ حلقه چاه و تعبیر و تفسیر داده های لرزه ای صورت پذیرفته و مدل های سرعت فشاری و برشی از مدل های زمین آماری ترکیبی، تعیین شده و با مدل های فرکتالی مورد مقایسه قرار گرفته اند. بر اساس داده های VSP، حداکثر سرعت لایه ای در محدوده ۲۹۰۰ - ۲۷۶۰ متر بر ثانیه در سمت شمال شرق مربوط به سازند گوتنیا می باشد. جهت مطالعات فشار شکست سازند نیز مدلسازی مکعب سرعت برشی با استفاده از مغزه های چاه اکتشافی و نگار سرعت برشی انجام شده که مکعب نهایی با ضریب همبستگی ۰/۹۵ برای داده های نگار سرعت برشی حاصل از داده های تخلخل، لیتولوژی و داده های اصلی سرعت برشی DSI تعیین شد. مقادیر نهایی مقاومت صوتی وارون سازی شده در اعماق بیشتر میدان اکثراً در محدوده ۱۵۰۰-۸۰۰۰ متر بر ثانیه در گرم بر سانتی متر مکعب می باشد که در محدوده سازند های آهکی می تواند قرار گیرد. بر اساس محاسبه ماتریس لوگرشیو حاصل از مدل فرکتالی مقدار حجم، بیشترین میزان تطبیق نهایی در بازه های سنگ آهک غالب به میزان ۰/۷۴ محاسبه شده است، که نشان از تطابق بالای مدل مکعب سرعت فشاری با استفاده از ترکیب شبیه سازی گوسی متوالی توام با کوکریجینگ و مقاومت صوتی حاصل از وارون سازی می باشد. مطالعات عدم قطعیت مکعب نهایی سرعت فشاری حدود ۵۰ درصد می باشد که با توجه به تعداد زیاد چاه ها قابل قبول است.

کلمات کلیدی: آنالیز لرزه ای، مدلسازی سرعت لرزه ای، مکعب سرعت فشاری، وارون سازی مقاومت صوتی، فشار سازندی، مدل فرکتالی سرعت- حجم.